

# ELLA: Exploration through Learned Language Abstraction

Suvir Mirchandani<sup>1</sup> Siddharth Karamcheti<sup>1</sup> Dorsa Sadigh<sup>1</sup>

## Abstract

Building agents capable of understanding language instructions is critical to effective and robust human-AI collaboration. Recent work focuses on training these instruction following agents via reinforcement learning in environments with synthetic language; however, these instructions often define long-horizon, sparse-reward tasks, and learning policies requires many episodes of experience. To this end, we introduce ELLA: Exploration through Learned Language Abstraction, a reward shaping approach that correlates high-level instructions with simpler low-level instructions to enrich the sparse rewards afforded by the environment. ELLA has two key elements: 1) A termination classifier that identifies when agents complete low-level instructions, and 2) A relevance classifier that correlates low-level instructions with success on high-level tasks. We learn the termination classifier offline from pairs of instructions and terminal states. Notably, in departure from prior work in language and abstraction, we learn the relevance classifier online, *without* relying on an explicit decomposition of high-level instructions to low-level instructions. On a suite of complex grid world environments with varying instruction complexities and reward sparsity, ELLA shows a significant gain in sample efficiency across several environments compared to competitive language-based reward shaping and no-shaping methods.

## 1. Introduction

A long-standing goal for robotics and embodied agents is to build systems that can perform tasks specified in natural language (Tellex et al., 2011; Thomason et al., 2015; Hermann et al., 2017; Anderson et al., 2018; Karamcheti et al.,

<sup>1</sup>Department of Computer Science, Stanford University, Stanford, CA. Correspondence to: Suvir Mirchandani <suvir@cs.stanford.edu>, Siddharth Karamcheti <skaramcheti@cs.stanford.edu>.

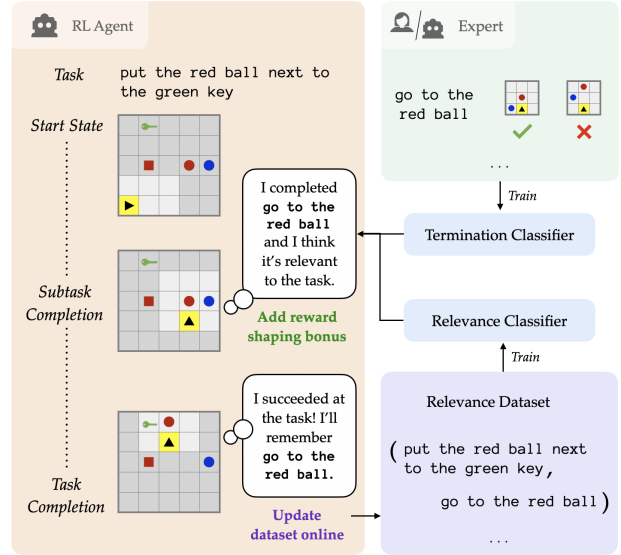


Figure 1. Our method incentivizes an RL agent (highlighted in yellow) to complete low-level language tasks relevant to its current task, using language abstractions learned online.

2020; Shridhar et al., 2020; Bisk et al., 2020). Central to the promise of language is in its ability to cleanly specify complex, multi-step instructions. Instructions like *make a cup of coffee* define long-horizon tasks as *abstractions* over lower-level components—simple instructions like *pick up a cup* or *turn on the coffee maker*. The key to natural and seamless human-AI collaboration is in finding a way to leverage these abstractions with the goal of amplifying the sample efficiency and generalization potential of our autonomous agents.

One way to do this is through the lens of *instruction following*, which can be framed in several ways. One common framing—and the one we use in this work—is via reinforcement learning (RL): an agent is given a start state, a language instruction, and a corresponding reward function to optimize that usually denotes termination (Hermann et al., 2017; Misra et al., 2017). RL is useful in developing agents that can solve moderately challenging tasks by exploring the environment and receiving reward signals; however, such approaches are often not sample efficient (Chevalier-Boisvert et al., 2019). Especially in the case of complex, highly

compositional language instructions, RL agents can fail to make progress quickly—or at all. There are several reasons for poor performance in these settings; paramount is that in many environments, these complex instructions are tied to sparse reward functions that only provide signal upon completion of the high-level task, which drastically hurts sample efficiency. For example, seeing a reward for an instruction like *make a cup of coffee* would require already having turned on the coffee maker, which could itself be a difficult task. Such “bottleneck” states, which have zero intermediate reward, complicate exploration and learning (McGovern & Barto, 2001; Stolle & Precup, 2002).

Our goal is to improve sample efficiency for instruction following agents operating in sparse reward settings. Driving our approach is using the principle of *abstraction*—the fact that complex instructions entail simpler ones—to guide exploration. Consider our running coffee example; we would like to guide the agent to explore in a structured fashion, learning low-level behaviors first (*pick up a cup, turn on the coffee machine*) building up to solving the high-level task. To do this, we frame our problem via *reward shaping*, the general technique of supplying auxiliary rewards to guide learning (Randløv & Alstrøm, 1998; Ng et al., 1999).

Our approach, Exploration through Learned Language Abstraction (ELLA) provides intermediate rewards to an agent for completing relevant low-level behaviors as it tries to solve a complex, sparse reward task (Figure 1). Notably, our approach 1) learns to identify the set of low-level primitives helpful for a high-level language task *online*, and 2) does not require a strict hierarchical decomposition of language instructions into these primitives. Rather, ELLA uses low-level instructions to support agents performing complex tasks, bonusing agents as they complete *relevant* low-level behaviors. This contract is simple and general; prior work (Andreas et al., 2017; Jiang et al., 2019) assumes a strict contract over how high-level instructions decompose, with each high-level task comprised of running out a series of low-level policies. This is only possible when given access to the full set of primitive behaviors ahead of time, and fails when new actions or further exploration is necessary.

In order to bonus agents as they complete relevant subtasks, ELLA assumes access to a set of low-level language instructions and their corresponding termination states, similar to the data assumed in Bahdanau et al. (2019). While collecting this data for complex, high-level tasks may require time and effort (and even then, require many more examples to generalize from), assuming annotations for low-level instructions is more tractable. Humans can quickly provide annotations for instructions like *pick up the cup* or *open the cupboard*, or even build tools for automatically generating such examples. Generally, dealing with simple, primitive instructions is a common way to simplify the problem of

interpreting high-level instructions (Jia & Liang, 2016; Arumugam et al., 2017; Wang et al., 2017; Karamcheti et al., 2020). In our case, these low-level primitives provide the basis for reward shaping.

Reward shaping in general is difficult, often requiring heuristic approaches for tuning certain hyperparameters that can critically impact performance (Goyal et al., 2019a). Our approach is similar in this regard, in that a critical hyperparameter that needs to be controlled for is the magnitude of the intermediate rewards. However, instead of using ad hoc methods for tuning this value, we provide a simple and systematic approach to determining a reasonable range for this value that generalizes across tasks. We empirically validate our abstraction-based reward shaping framework on a series of synthetic discrete action tasks via the BabyAI platform (Chevalier-Boisvert et al., 2019). We compare against a standard RL baseline as well as to a strong language-based reward shaping approach (Goyal et al., 2019a), and find that our method leads to substantial gains in sample efficiency across a variety of instruction following tasks.

## 2. Related Work

We build upon a large body of work that examines language in the context of deep reinforcement learning (Luketina et al., 2019) with a focus on methods for instruction following, leveraging hierarchy, and reward shaping.

**Instruction Following.** In the context of embodied agents instruction following focuses on the automated execution of language commands in simulated or real environments (Kollar et al., 2010; Tellex et al., 2011; Anderson et al., 2018). Approaches range from imitation learning (Wang et al., 2019) to inverse reinforcement learning (Fu et al., 2019). We focus on the reinforcement learning paradigm (Misra et al., 2017; Chevalier-Boisvert et al., 2019), where the agent learns a policy conditioned on the language instruction in a Markov decision process (MDP).

Even simple instruction following problems are difficult to learn (Lynch & Sermanet, 2020), which has made 2D environments important test-beds for new learning methods (Andreas et al., 2017; Yu et al., 2017; Chevalier-Boisvert et al., 2019). Such environments, which are procedurally-generated, are useful because they decouple exploration from the problem of perception, and demand policies that do not overfit to narrow regions in the state space (Campero et al., 2020; Cobbe et al., 2020).

We use BabyAI (Chevalier-Boisvert et al., 2019) as the platform for our tasks. Like other instruction following environments, BabyAI’s language is synthetic. These environments are important, scalable starting points for new instruction following approaches, since deep RL remains

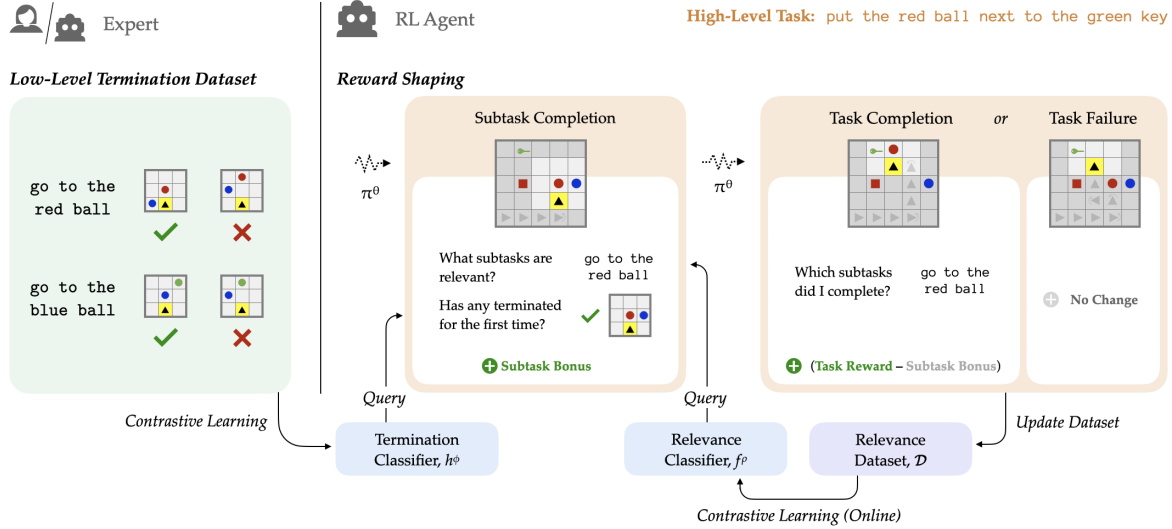


Figure 2. In this example, an expert provides examples of when low-level *go to* tasks are and are not solved, and the agent trains a termination classifier. During policy learning, the agent rewards itself for completing *go to* subtasks—specifically, those which are relevant to its current high-level task. It stores successful experiences to learn to correlate low-level *go to* tasks with high-level *put next* tasks.

sample-inefficient but has the potential to flexibly deal with complex environments (Hill et al., 2020). Simplified environments also make investigating concepts such as language abstraction possible, and these concepts can generalize to real human-AI interactions (Wang et al., 2017; Karamcheti et al., 2020). We describe our setup in Section 5.

**Hierarchical and Language-Structured Policies.** A large body of work in hierarchical RL studies temporal abstractions of MDPs, where policies are designed or learned at multiple levels of hierarchy (Sutton et al., 1999). Recent works have made the connection to language: for example, high-level policies can act over the space of low-level instructions (Jiang et al., 2019). Other hierarchical language techniques include learning models that predict symbolic representations of reward functions at different granularities (Arumugam et al., 2017; Karamcheti et al., 2017), and compositional approaches like policy sketches (Andreas et al., 2017) and modular control (Das et al., 2018), methods that explicitly decompose high-level instructions into sequences of predefined low-level instructions, or subtasks.

In this work, we use language hierarchically, but *without* the strict decomposition assumption made by prior work: we do not assume high-level tasks are strict compositions of low-level tasks. Doing so would unrealistically restrict our notion of abstraction. Rather, we assume that a high-level instruction is “supported” by low-level language even if it is not fully factorizable into low-level instructions. Say the low-level task space consists of *go to* “ $x$ ” instructions: *go to the red ball*, *go to the blue ball*, etc. The instruction *go to the red ball and then go to the blue ball* can be fully factorized into the low-level task set. On the other hand, the

instruction *put the red ball next to the green key* is supported by *go to the red ball*, but it also requires picking up and putting down the ball—actions not covered by the low-level *go to* tasks. This makes it difficult to use explicitly modular approaches (Arumugam et al., 2017; Andreas et al., 2017; Das et al., 2018) out of the box; instead need to be able to explore using a mixture of these low-level instructions *as well as* primitive actions. A further distinguishing factor of our method relative to prior work is that we do not require high-level task decompositions be provided *a priori*. We expand on these features in Section 3.

**Language and Reward Shaping.** Reward shaping is a general technique for supplying auxiliary rewards in order to guide an agent’s learning process. Certain types of reward transformations, such as potential-based rewards, do not change the optimal policy but can impact sample efficiency (Ng et al., 1999). Prior work has applied reward shaping to language-based instruction following settings. Goyal et al. (2019a) train a classification network on (trajectory, language) data to predict if a trajectory (parameterized by action frequencies) matches a language description, and evaluate the network at every time step to form a potential-based reward shaping function. They evaluate their method on Montezuma’s Revenge, which is a complex task, but with a static, deterministic layout that does not speak to the generalization potential of such methods. Relatedly, Waytowich et al. (2019) use a narration-based approach, where high-level tasks are explicitly broken down into low-level tasks as narrations. Finally, Misra et al. (2017) use a shaping function based on spatial distance to goals specified in language, but require the location of the goal to be known. In this work, we use the same high level principle—language

can yield useful intermediate rewards—but do not make the restrictive assumptions of prior work about the environment or the way tasks are structured.

**Other Forms of Guidance.** Several other methods exist for improving the sample efficiency of RL in sparse reward settings. These methods are orthogonal to our approach, but we see potential for combining these methods with ours. One popular technique is hindsight experience replay (HER), in which failed trajectories are stored in a replay buffer and relabeled with new goals that get nonzero reward (Andrychowicz et al., 2017). Jiang et al. (2019) extend the method to hierarchical language settings, assuming a mapping from states to corresponding goals. Cideron et al. (2019) learn this mapping alongside policy training using the environment reward as supervision. Another technique for improving sample efficiency is through intrinsic motivation (Schmidhuber, 1991; Pathak et al., 2017; Burda et al., 2019). In general, these methods instantiate reward shaping to incentivize accessing novel or unpredictable parts of the state space via intrinsic rewards, and they can be extended to language-conditioned settings as well (Colas et al., 2020).

### 3. Problem Statement

We consider an augmented MDP  $\mathcal{M}$  defined by the tuple  $(\mathcal{S}, \mathcal{A}, T, R, \mathcal{G}, \gamma)$  where the definitions of  $\mathcal{S}, \mathcal{A}, T$  and  $\gamma$  are standard.  $\mathcal{G}$  is a set of language instructions, from which an instruction  $g$  is drawn, and  $R : \mathcal{S} \times \mathcal{A} \times \mathcal{G} \rightarrow [0, 1]$  represents the state-action reward given some  $g$ . Via RL, we wish to find some policy  $\pi : \mathcal{S} \times \mathcal{G} \rightarrow \mathcal{A}$  that maximizes the expected discounted return.

We specifically consider cases where  $\mathcal{M}$  has a finite horizon  $H$  and  $R$  is sparse with respect to goal-completion, making exploration difficult. Our aim is to construct a reward transformation  $R \rightarrow R'$  which is policy invariant with respect to the original MDP (i.e. an optimal policy for  $\mathcal{M}' = (\mathcal{S}, \mathcal{A}, T, R', g, \gamma)$  is also optimal in  $\mathcal{M}$  and vice versa), and which provides the agent strong supervisory signal that leads to sample-efficient exploration.

We assume access to low-level instructions  $\mathcal{G}_\ell$  such that every  $g \in \mathcal{G}$  is supported by some  $g_\ell \in \mathcal{G}_\ell$ . (For example:  $g = \text{wash the dishes}$  is supported by  $g_\ell = \text{pick up a dish}$ .) We assume that examples of the corresponding termination states are easy to obtain—via a human expert or automation. This is reasonable for simple low-level task sets like the *go to* tasks in Figure 2. However, it may be less feasible in domains where data collection is time-consuming or costly and the environment is hard to simulate; we address this further in Section 7.

In our experiments, we use partially observable environments, with recurrent neural policies that ingest sequences

---

#### Algorithm 1 PPO with Reward Shaping via ELLA

---

**Input:** Initial policy params.  $\theta_0$ , relevance function params.  $\rho_0$  and update rate  $n$ , and low-level task bonus  $\lambda$   
 Initialize  $\mathcal{D} = \{g : \mathcal{G}_\ell \text{ for all } g \in \mathcal{G}\}$ .  
**for**  $k = 0, 1, \dots$  **do**  
     Collect partial trajectories  $\{\tau_i\}$  with  $\pi_k^\theta$ . Shape reward with  $+\lambda$  whenever  $h^\phi$  predicts any  $g_\ell$  terminates.  
     **for** each successful trajectory  $\tau$  and goal  $g$  **do**  
         Set final shaped reward to neutralize prior rewards.  
         Set  $\mathcal{D}[g]$  to  $\mathcal{D}[g] \cap \{g_\ell : g_\ell \text{ terminated in } \tau\}$ .  
     **end for**  
     Update  $\theta_{k+1}$  using PPO objective with shaped rewards.  
     Every  $n$  iterations, update  $\rho_{k+1}$  to minimize cross entropy loss on  $\mathcal{D}$ .  
**end for**

---

of observations  $(o_1, o_2, \dots, o_t)$  rather than single states  $s_t$ . Though we describe the fully observable setting above, the extension to the partially observable case is straightforward.

## 4. ELLA

We present ELLA, our reward shaping framework for guiding exploration using learned language abstractions.<sup>1</sup> Figure 2 provides a graphical overview of ELLA, while Algorithm 1 breaks it down systematically. Our approach rewards an agent when it has completed low-level tasks that support a given high level task. To do this, it needs to predict 1) when a low-level task *terminates* and 2) when a low-level task is *relevant*. Section 4.1 describes how we build the termination classifier while Section 4.2 describes how we train a relevance classifier, which we learned online during RL. Finally, Section 4.3 provides the details of our reward shaping scheme, which bonuses the agent for exploring states that satisfy relevant low-level tasks.

### 4.1. Learning a Low-Level Termination Classifier

We train a binary termination classifier  $h^\phi : \mathcal{S} \times \mathcal{G}_\ell \rightarrow \{0, 1\}$  parameterized by  $\phi$  to predict if a low-level task  $g_\ell \in \mathcal{G}_\ell$  terminates in a particular state  $s \in \mathcal{S}$ . We assume access to  $\mathcal{G}_\ell$  as well as positive and negative examples of low-level task termination states. This dataset could be provided by a human annotator or created automatically; while providing demonstrations of high-level tasks (e.g., *make a cup of coffee*) across varied environments is costly, doing so for low-level tasks (e.g., *pick up the mug*, *open the cupboard*) which are shorter, simpler, and more generalizable, is more feasible. To represent  $h^\phi$ , we use an adapted version of the architecture in (Chevalier-Boisvert et al., 2019) which merges state and language representations using feature-wise linear modulation (FiLM) (Perez et al., 2018).

<sup>1</sup>Code at <https://github.com/Stanford-ILIAD/ELLA>



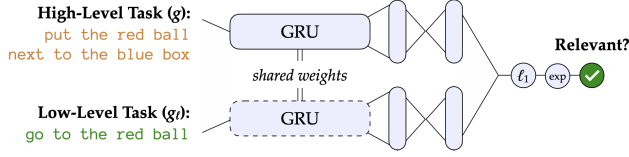


Figure 3. ELLA’s relevance classifier identifies whether a high-level task abstracts over a particular low-level task.

LOW-LEVEL TASK	EXAMPLE	
GoTo-ROOM (G1)	<i>go to a red ball</i>	
GoTo-MAZE (G2)	<i>go to a red ball</i>	
OPEN-MAZE (O2)	<i>open the green door</i>	
PICK-MAZE (P2)	<i>pick up the blue box</i>	
HIGH-LEVEL TASK	EXAMPLE(S)	$\mathcal{G}_\ell$
PUTNEXT-ROOM	<i>put the red ball next to the green key</i>	G1
PUTNEXT-MAZE	<i>put the red ball next to the green key</i>	G2
UNLOCK-MAZE	<i>open the green door</i>	P2
OPEN&PICK-MAZE	<i>open the yellow door and pick up the blue box</i>	O2, G2
COMBO-MAZE	<i>put next, open, pick</i>	G2
SEQUENCE-MAZE	<i>pick up a purple key and then put the grey box next to the yellow box</i>	G2

Table 1. Sample instructions for our low- and high-level tasks.

## 4.2. Learning the Relevance Classifier

Our reward shaping approach also needs to evaluate the relevance of a low-level instruction in addition to being able to classify termination. The relevance mapping from  $\mathcal{G}$  to  $\mathcal{P}(\mathcal{G}_\ell)$  (the power set of  $\mathcal{G}_\ell$ ) is initially unknown to the agent. We refer to the output of this mapping as a decomposition of  $g$ , but note again that it need not be a *strict* decomposition. We propose that this mapping is represented by a separate binary relevance classifier  $f^\rho : \mathcal{G} \times \mathcal{G}_\ell \rightarrow \{0, 1\}$  learned online during policy training. The output of  $f^\rho$  indicates whether a particular  $g_\ell \in \mathcal{G}_\ell$  is relevant to some  $g \in \mathcal{G}$ . We use a Siamese network to represent  $f^\rho$  (Figure 3).

**Training the Relevance Classifier.** Suppose  $\mathcal{D}$  already contains tuples  $(g, S)$  where  $g \in \mathcal{G}$  and  $S \in \mathcal{P}(\mathcal{G}_\ell)$ . Each  $S$  is an estimate of the oracle decomposition  $\bar{S}$  of a particular  $g$ . For every  $g$  in  $\mathcal{D}$ , we enumerate negative examples of relevant subtasks from  $\mathcal{G}_\ell \setminus S$  and accordingly oversample positive examples from  $S$  and optimize a binary cross entropy objective on  $\mathcal{D}$ .

**Collecting Relevance Data Online.** For every successful trajectory of some  $g$  we encounter during RL training, we record the low-level instructions which terminated. That is,

we relabel the steps in the trajectory and use  $h^\phi$  to determine which low-level instructions were completed (if any), yielding an estimate  $\hat{S}$  of the true decomposition  $\bar{S}$ . If  $\mathcal{D}$  already contains an estimate  $S$  for  $g$ , we use a simple heuristic method for deduplicating the multiple decomposition estimates: intersect  $S$  and  $\hat{S}$ . As the agent completes more successful trajectories, decompositions in  $\mathcal{D}$  are more likely to get revisited.

**Intuition for Deduplication.** Intuitively, this method for deduplication denoises run-specific experiences, and distills the decomposition estimate in  $\mathcal{D}$  for a given  $g$  to only those  $g_\ell$  that are shared among various successful runs of  $g$ . Consider the high-level instruction  $g = \text{put the red ball next to the blue box}$ ; successful runs at the beginning of training could highlight *go to the red ball* and irrelevant *go to low-level instructions*. As  $\pi^\theta$  improves, so do the decomposition estimates. Later runs may highlight only *go to the red ball*. Taking the intersection would yield only the common low-level instruction *go to the red ball* as our final estimate  $S$ . This approach also helps to deal with false positives of  $h^\phi$  by effectively boosting the estimate across multiple runs. If deduplication produces a null intersection, which may happen due to false negatives of  $h^\phi$ , we err on the side of using the latest decomposition estimate. If we assume  $h^\phi$  has perfect accuracy, the intersection will never be null, and the continual intersections will reflect the set of completed  $g_\ell$  common to all the successful runs of  $g$ . For an initialization conducive to deduplication and that provides  $\pi^\theta$  strong signal from the beginning of training, we initialize  $f^\rho$  to predict that all  $g_\ell$  are relevant for any  $g$ .

## 4.3. Shaping Rewards

We now describe the shaped reward function  $R'$  which relies on  $h^\phi$  and  $f^\rho$ .  $R'$  provides a bonus  $\lambda$  whenever a relevant low-level task terminates. We do this by relabeling the current  $(s_t, a_t, r_t, s_{t+1})$  with every  $g_\ell$  and using  $h^\phi$  to predict low-level task termination, and  $f^\rho$  to predict relevance.

Critically, we do not want the shaping transformation from  $R \rightarrow R'$  to be vulnerable to the agent getting “distracted” by the shaped reward (reward hacking), as in [Randløv & Alstrøm \(1998\)](#) where an agent learns to ride a bicycle in a circle around a goal repeatedly accruing reward. To prevent this, we cap the bonus per low-level instruction per episode to  $\lambda$  to prevent cycles. More generally, we want  $R'$  to be *policy invariant* with respect to  $\mathcal{M}$ : it should not introduce any new optimal policies, and it should retain all the optimal policies from  $\mathcal{M}$ . Policy invariance is a useful property ([Ng et al., 1999](#)): we do not want to reward a suboptimal trajectory (such as one that repeatedly completes a low-level instruction) more than an optimal trajectory in  $\mathcal{M}$ , and policy invariance guarantees this.

We establish two desiderata for  $R'$  (Behboudian et al., 2020): (a) The reward transformation should be policy invariant with respect to  $\mathcal{M}$  for states from which the task is solvable, and (b)  $R'$  should improve sample efficiency by encouraging subtask-based exploration.

We describe any trajectory that solves the high-level task as *successful*, regardless of whether they do so optimally, and any other trajectories as *unsuccessful*. To satisfy our desiderata, we choose  $R'$  such that successful trajectories get the same return under  $\mathcal{M}$  and  $\mathcal{M}'$ , and that unsuccessful trajectories get lower returns under  $\mathcal{M}'$  than trajectories optimal in  $\mathcal{M}$ . We will describe and intuitively justify each of these choices with respect to (a) and (b). We follow this discussion with a proof sketch that  $R'$  satisfies (a) and empirical evidence that it satisfies (b).

**Neutralization in Successful Trajectories.** We neutralize shaped reward in successful trajectories—that is, subtract the shaped reward at the final time step—so that successful trajectories gets the same return under both  $R'$  and  $R$ .

More specifically, let  $U(\tau)$  and  $U'(\tau)$  refer to the cumulative discounted return of a successful trajectory  $\tau$  under  $R$  and  $R'$  respectively. If  $\tau$  has  $N$  steps, the sparse reward under  $R$  is  $U(\tau) = \sum_{t=1}^N \gamma^t R(s_t, a_t) = \gamma^N r_N$ . Under  $R'$ , if  $T_S$  is the set of the time steps at which a  $\lambda$  bonus is applied, we set  $r'_N$  to  $r_N - \sum_{t \in T_S} \gamma^{t-N} \lambda$ . This is the value required to neutralize the intermediate rewards, such that  $U'(\tau) = \gamma^N r'_N = U(\tau)$ . (As an implementation detail, note that we cap the bonus per time step to  $\lambda$ —if multiple low-level language instructions terminate at a single state, only a bonus of  $\lambda$  is applied.)

Theoretically, we could apply neutralization to *all* trajectories, not just successful ones, and we would satisfy property (a) (Grzes, 2017). However, this is harmful to property (b), because unsuccessful trajectories would result in zero return: a negative reward at the last time step would negate the subtask rewards, hurting any boost in sample efficiency.

#### Tuning $\lambda$ to Limit Return in Unsuccessful Trajectories.

Any successful trajectory gets the same return under  $R'$  as under  $R$  because of neutralization. By choosing  $\lambda$  carefully, we can additionally satisfy the property that any unsuccessful trajectory gets a lower return under  $R'$  than any trajectory chosen by an optimal policy  $\pi_{\mathcal{M}}^*$  in  $\mathcal{M}$ .

To achieve this, we need  $\lambda$  to be sufficiently small. Assume that a trajectory  $\tau$  chosen by  $\pi_{\mathcal{M}}^*$  takes no longer than  $M$  time steps to solve any  $g$ . In the worst case,  $M = H$ , and  $U(\tau)$  would be  $\gamma^H r_H$ . If  $T_S$  is the set of the time steps at which  $R'$  provides  $\lambda$  bonuses,  $U'(\tau)$  would be  $\lambda \sum_{t \in T_S} \gamma^t$ . We can upper bound  $\sum_{t \in T_S} \gamma^t$  with  $|\mathcal{G}_\ell|$ . Then, the follow-

ing inequality is sufficient for maintaining (a):

$$\lambda < \frac{\gamma^H r_H}{|\mathcal{G}_\ell|}, \quad (1)$$

where  $r_H$  is the value of a sparse reward if it were attained at time step  $H$ . We provide a more thorough justification in Section 4.4. Note that  $\lambda$  and the sparse reward can be scaled by a constant if  $\lambda$  is otherwise too small to propagate as a reward.

An important feature of our work is the realization that we can make this bound less conservative through minimal knowledge about the optimal policy and the environment (e.g., knowledge about the expected task horizon  $M$ , or a tighter estimate of the number of subtasks available in an environment instance). The corresponding values of  $\lambda$  can empirically lead to faster learning (Section 6.1). At a minimum, reasoning over the value of  $\lambda$  using via (1) provides a generalizable way to incorporate this technique across a variety of different settings in future work.

#### 4.4. Proof of Policy Invariance

In this section, we sketch the proof of the policy invariance of our reward transformation. We begin with the goal-conditioned MDP  $\mathcal{M} = (\mathcal{S}, \mathcal{A}, T, R, \mathcal{G}, \gamma)$ , where  $T : \mathcal{S} \times \mathcal{A} \times \mathcal{S} \rightarrow [0, 1]$  and  $R : \mathcal{S} \times \mathcal{A} \times \mathcal{S} \times \mathcal{G} \rightarrow [0, R_{max}]$ .  $R$  is sparse. Let  $\tilde{\mathcal{M}}$  be an augmented MDP  $(\tilde{\mathcal{S}}, \mathcal{A}, \tilde{T}, \tilde{R}, \mathcal{G}, \gamma)$  which stores state histories: that is,  $\tilde{s}_t = (s_t, h_{0:t-1})$ .  $\tilde{T} : \tilde{\mathcal{S}} \times \mathcal{A} \times \tilde{\mathcal{S}} \rightarrow [0, 1]$  is defined as  $\tilde{T}(\tilde{s}_t, a_t, \tilde{s}_{t+1}) = T(s_t, a, s_{t+1}) \cdot \mathbb{1}[h_{0:t} = (h_{0:t-1}, s_t)]$ .  $\tilde{R}$  is defined similarly to reflect consistency between histories. The transformation from  $\mathcal{M}$  to  $\tilde{\mathcal{M}}$  does not affect optimal policies because we are simply appending history information to the state without affecting the dynamics. We now use  $\tilde{\mathcal{M}}$  (instead of  $\mathcal{M}$ ) to show policy invariance with a given shaped MDP  $\mathcal{M}'$ , as we describe below.

Consider a shaped MDP  $\mathcal{M}' = (\tilde{\mathcal{S}}, \mathcal{A}, \tilde{T}, R', \mathcal{G}, \gamma)$  where  $R' : \tilde{\mathcal{S}} \times \mathcal{A} \times \tilde{\mathcal{S}} \rightarrow [0, 1]$  is defined as  $R'(\tilde{s}_t, a_t, \tilde{s}_{t+1}) = \tilde{R}(\tilde{s}_t, a_t, \tilde{s}_{t+1}) + \ell(\tilde{s}_t, \tilde{s}_{t+1})$  where  $\ell : \tilde{\mathcal{S}} \times \tilde{\mathcal{S}} \rightarrow \mathbb{R}$  represents the low-level task bonuses (or neutralization penalty) going from state  $\tilde{s}_t$  to  $\tilde{s}_{t+1}$  as defined in Section 4.3. We first aim to show that the transformation from  $\tilde{\mathcal{M}}$  to  $\mathcal{M}'$  does not introduce new optimal policies—that is, any optimal policy in  $\mathcal{M}'$  is also optimal in  $\tilde{\mathcal{M}}$ .

Let  $\hat{\pi}_{\tilde{\mathcal{M}}}(\tilde{s}) = \pi_{\mathcal{M}'}^*(\tilde{s})$  where  $\pi_{\mathcal{M}'}^*$  is optimal in  $\mathcal{M}'$ . We will show this policy is also optimal in  $\tilde{\mathcal{M}}$ : that is,  $V_{\tilde{\mathcal{M}}}^{\hat{\pi}_{\tilde{\mathcal{M}}}}(\tilde{s}_t) = V_{\tilde{\mathcal{M}}}^*(\tilde{s}_t)$  for all  $\tilde{s}_t$ . Since  $\tilde{R}$  is nonnegative and sparse, we only need to consider states  $\tilde{s}_t$  at which the value could possibly be positive: those from which the task is solvable in at most  $H - t$  steps, where  $H$  is the horizon.

Assume the task is solvable in a minimum of  $k \leq H - t$  steps (using an optimal policy in  $\tilde{\mathcal{M}}$ ). We can reason about

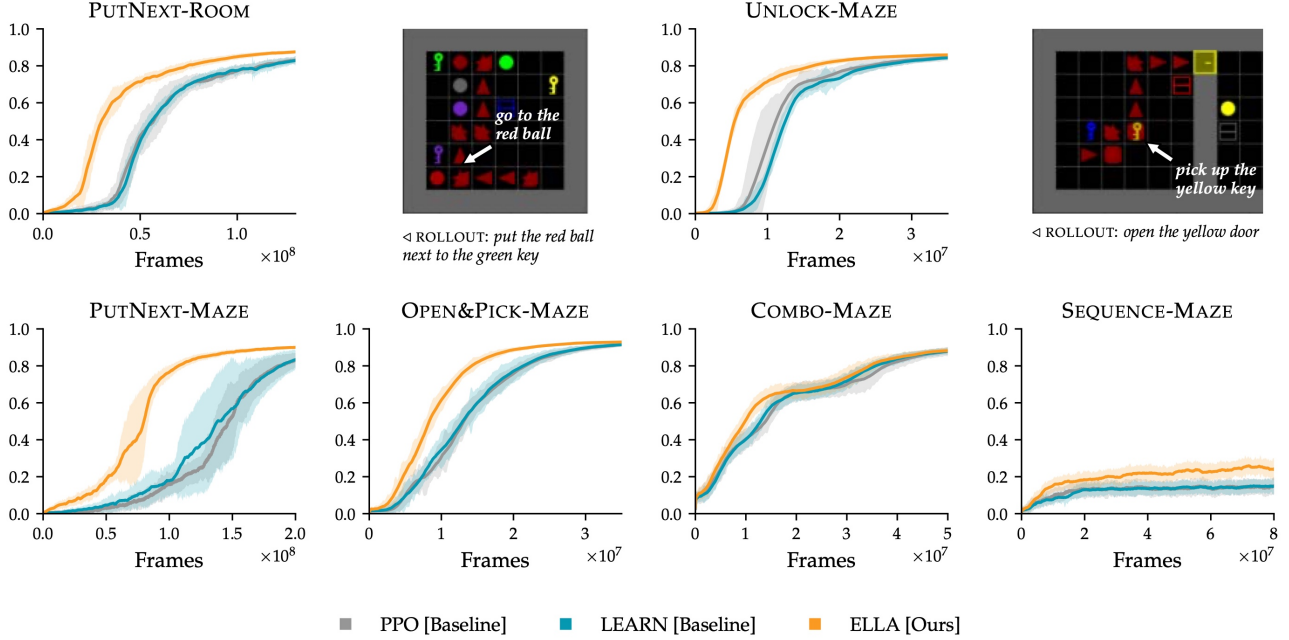


Figure 4. Average reward for ELLA and baselines in six environments, with error regions to indicate standard deviation over three random seeds. Example rollouts in the PUTNEXT-ROOM environment and UNLOCK environment illustrate the final policy learned via ELLA, where the agent completes relevant low-level subtasks in order to solve the high-level task.

$\hat{\pi}_{\tilde{\mathcal{M}}}(\tilde{s}) = \pi_{\mathcal{M}'}^*(\tilde{s})$  by considering the various ways return could be accumulated in  $\mathcal{M}'$ , and which of those cases yields the maximum return.

(1) A policy could solve the task in  $j \geq k$  steps while solving subtasks at timesteps  $T_S$ , and receive a discounted future return of  $\sum_{t' \in T_S; t' \geq t} \gamma^{t'-t} \lambda + \gamma^j (R_{max} - \sum_{t' \in T_S} \gamma^{t'-(t+j)} \lambda)$ .

(2) A policy could solve only subtasks at timesteps  $T_S$  and receive a discounted future return of  $\sum_{t' \in T_S; t' \geq t} \gamma^{t'-t} \lambda$ .

We can simplify the return in case (1) to  $\gamma^j R_{max} - \sum_{t' \in T_S; t' < t} \gamma^{t'-t} \lambda$ . The second term does not depend on actions taken after  $t$ ; thus, this case is maximized by completing the task in  $j = k$  steps.

Note that case (2) always gets smaller return than case (1): the first term,  $\sum_{t' \in T_S; t' \geq t} \gamma^{t'-t} \lambda$ , is the same as in case (1), and the second term in case (1) is strictly positive when we use the bound on  $\lambda$  from Section 4.3: that  $\lambda < \frac{\gamma^H R_{max}}{|\mathcal{G}_\ell|}$ .

Therefore, the maximum future return is achieved in case (1), specifically by a policy that solves the task in  $k$  steps, and we know that this policy exists. Thus  $V_{\tilde{\mathcal{M}}}^{\hat{\pi}_{\tilde{\mathcal{M}}}}(\tilde{s}_t) = \gamma^k R_{max} = V_{\mathcal{M}'}^*(\tilde{s}_t)$ , and so an optimal policy in  $\mathcal{M}'$  is also optimal in  $\tilde{\mathcal{M}}$ . In order to show the reverse, we can use similar logic to show that any optimal policy in  $\tilde{\mathcal{M}}$  acts optimally in  $\mathcal{M}'$  for any state  $\tilde{s}_t$  where the task is solvable

in a minimum of  $k \leq H - t$  steps; actions towards solving the task most quickly are also optimal in  $\mathcal{M}'$ . Together, this shows policy invariance between  $\tilde{\mathcal{M}}$  and  $\mathcal{M}'$  for the set of states  $\tilde{s}_t$  where the task is solvable.

## 5. Experiments & Results

**Experimental Setup.** We run our experiments in BabyAI (Chevalier-Boisvert et al., 2019), a grid-world platform for instruction following, where an agent has a limited range of view and receives goal instructions such as *go to the red ball* or *open a blue door*. Grid worlds can consist of multiple rooms connected by a closed/locked door (e.g., the UNLOCK-MAZE environment in Figure 4). The action space  $\mathcal{A}$  consists of several navigation primitives (forward, pickup, etc.). Every task instance includes randomly placed distractor objects that agents can interact with. Rewards are sparse: agents receive a reward of  $1 - 0.9 * \frac{t}{H}$  where  $t$  is the current time step only upon succeeding at the high-level goal. If the goal is not reached, the reward is 0. By default, the reward function gets scaled up by a factor of 20.

We evaluate our reward shaping framework using Proximal Policy Optimization (PPO) (Schulman et al., 2017), but note that ELLA is agnostic to the RL algorithm used. We compare to PPO without shaping, as well as to LEARN, a prior method on language-based reward shaping (Goyal et al., 2019a) that provides rewards based on the predicted

relevance of action frequencies in the current trajectory to the current instruction.

We focus on several high- and low-level tasks. Table 1 describes each task, with examples. ROOM levels consist of a single  $7 \times 7$  grid, while MAZE levels contain two such rooms, connected by a door; agents may need to open and pass through the door multiple times to complete the task. In the UNLOCK environment, the door is “locked,” requiring the agent to hold a key of the same color as the door before opening it, introducing significant bottleneck states (McGovern & Barto, 2001; Stolle & Precup, 2002). Our six high-level tasks differ on three axes: *sparsity* of the high-level task, *similarity* of the low- and high-level tasks, and *compositionality* of the tasks in  $\mathcal{G}$ —the number of  $g_\ell \in \mathcal{G}_\ell$  relevant to some  $g$ . We use these axes to frame our understanding of how ELLA performs in different situations.

We used a combination of NVIDIA Titan and Tesla T4 GPUs to train our models. We ran 3 seeds for each of the 3 methods in each environment, with runs taking 1 to 6 days.

**Results.** Figure 4 presents learning curves for ELLA, LEARN, and PPO (without shaping) across the six environments. We explain our results in the context of the three axes described above.

### 1. How does ELLA perform on tasks of varying sparsity?

In both single room (PUTNEXT-ROOM) and two room (PUTNEXT-MAZE) environments, ELLA induces gains in sample efficiency, using GOTO as  $\mathcal{G}_\ell$ . Relative gains are larger for the bigger environment because reward signals are more spatially sparse and so spatial subgoals—visiting relevant objects—help the agent navigate.

Another degree of sparsity comes from bottleneck states: for example, in the UNLOCK environment, the agent must pick up a key of the corresponding color (the bottleneck) before it can successfully open a colored door and see reward. Without shaping, random exploration rarely passes such bottlenecks. However, in this experiment, ELLA rewards picking up keys, via the PICK low-level instruction, quickly learning to correlate picking keys of the correct color with successfully unlocking doors, allowing agents to navigate these bottlenecks and improving sample efficiency.

### 2. How does ELLA perform when the low-level tasks are similar to the high-level task?

In the COMBO environment, tasks consist of multiple types of instructions such as *put the red ball next to the green box*, *open the green door*, and *pick up the blue box*. The latter instructions require minimal exploration beyond “going to” the object in question. That is, the low-level task GOTO is more similar to this high-level task set than in the other environments such as PUTNEXT. As a result, in the COMBO

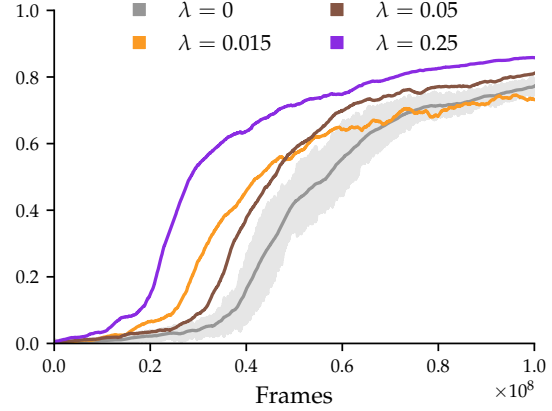


Figure 5. Average reward in PUTNEXT-ROOM for various values of  $\lambda$ . Smaller values are more conservative but potentially less helpful than larger values.  $\lambda = 0$  indicates no shaping; for this case, we show an error region over three random seeds.

environment, ELLA does not increase in sample efficiency. However, it notably does not perform *worse* than baselines: the exploration it encourages is not harmful, but is simply not helpful. This is expected as subtasks are relatively similar to many high-level tasks, and achieving them is about as difficult as exploring the correct subtasks.

### 3. How does ELLA perform when the high-level tasks are compositional and diverse?

We test ELLA on OPENANDPICKUP using *two* low-level instruction families, OPEN and GOTO. The instruction *open the yellow door and pick up the blue box* abstracts over *go to the yellow door*, *open the yellow door*, and *go to the blue box*. Although learning the relevance classifier becomes more difficult with more compositional instructions, the boost in sample efficiency provided by ELLA remains.

Similarly, the SEQUENCE environment has a combinatorially-large number of compositional instructions: it requires two of *put next*, *open*, and *pick up* to be completed in the correct order. It has over 1.5 million instructions compared to the other high-level tasks which range from 300 to 1500 instructions. Although the exploration problem is very difficult, we see marginal gains from ELLA; we discuss this further in Section 7.

## 6. Analyzing ELLA

In this section, we analyze two aspects of ELLA’s performance: the effect of different choices for the low-level task reward hyperparameter (Section 6.1), and the performance of the relevance classifier over an RL run (Section 6.2).



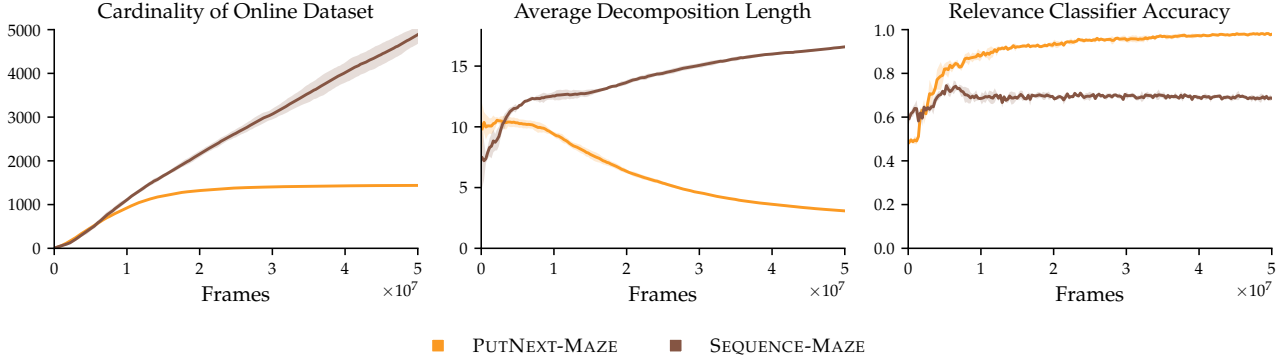


Figure 6. Three metrics to analyze ELLA’s performance over an RL run are the size of the online dataset  $\mathcal{D}$ , the average number of low-level instructions per high-level instruction in  $\mathcal{D}$  over time, and the accuracy of the relevance classifier on a balanced validation set. For PUTNEXT-MAZE, the relevance classifier improves as the decomposition estimates get less noisy and the online dataset converges to its largest size. For the challenging SEQUENCE-MAZE task, ELLA still incentivizes subtask completion, evidenced by the growing dataset and the high length of decompositions, but the decomposition estimates are noisy and the relevance classifier is less accurate.

### 6.1. Effect of the Low-Level Task Reward

Section 4.3 provides guidelines for choosing the value of the subtask reward  $\lambda$ : to summarize, we want to pick  $\lambda$  small enough that any unsuccessful trajectory—such as one that only completes subtasks and never finishes the high-level task—does not receive greater return than an optimal trajectory. We find that values of  $\lambda$  that egregiously violate policy invariance lead to unstable learning. In this section, we observe this effect in PUTNEXT-ROOM, by evaluating various values of  $\lambda$  determined using the multi-tier assumptions alluded to in Section 4.3. With no knowledge of the environment or the expert policy, the loosest bounds for  $M$  and  $|T_S|$  in (1) gives us a value of  $\lambda = 0.015$ . With the minimal assumption that the expert policy solves the task in under 100 steps, we arrive at  $\lambda = 0.05$ . For 40 steps, we arrive at  $\lambda = 0.25$ . Figure 5 compares learning curves for  $\lambda$ —the smallest being more conservative and not having a great effect on sample efficiency, and the largest illustrating the value of rewarding relevant subtasks. The results in Section 5 use  $\lambda = 0.25$  for PUTNEXT-ROOM, PUTNEXT, UNLOCK, and COMBO, and use  $\lambda = 0.5$  for OPEN&PICK and SEQUENCE (which have longer horizons  $H$ ).

### 6.2. Progress of the Relevance Classifier

The online relevance dataset and classifier provide transparency into the type of guidance that ELLA provides. Figure 6 focuses on PUTNEXT-MAZE and SEQUENCE-MAZE, and shows three metrics: the cardinality of  $\mathcal{D}$  over time, which we expect to increase and possibly converge; the average number of subtasks per high-level instruction in  $\mathcal{D}$ , which we expect to decrease as decomposition estimates improve; and the validation accuracy of  $f^p$  in classifying a balanced oracle set of subtask decompositions, which we

expect to increase if ELLA learns language abstractions.

For PUTNEXT-MAZE, the cardinality of  $\mathcal{D}$  grows and then converges (as the policy successfully completes all the tasks). This happens as the number of subtasks per high-level instruction decreases, the relevance classifier becomes very accurate, and from Figure 4, the policy improves in terms of average return. For the SEQUENCE-MAZE task, ELLA has marginal gains in performance compared to baselines (Figure 4). This is likely due to ELLA incentivizing general subtask completion, which is evidenced by the increasing size of the dataset and growing average length of the decompositions. However, the large number of diverse language instructions makes it difficult to estimate good decompositions via our deduplication method, and so it is difficult to learn the relevance classifier online.

## 7. Discussion and Future Work

**Limitations.** Our framework requires termination states for each low-level instruction. This assumption is similar to that made by Jiang et al. (2019) and Waytowich et al. (2019), and is weaker than the assumption made by the LEARN baseline of Goyal et al. (2019a), where full demonstrations are required. However, training accurate termination classifiers can require many examples—in this work, we used 15K positive and negative pairs for each low-level task. Ideally, these examples (or the tasks themselves) could be gathered without supervision. In its current form, our approach is less feasible in domains where collecting examples of terminating conditions for each low-level task is costly.

ELLA also experiences smaller gains in the SEQUENCE-MAZE environment, which has a large number of highly compositional and diverse instructions. One explanation is that our method of collecting data for the relevance classifier

(Section 4.2) performs better when the agent sees the same instruction multiple times (and deduplicates appropriately), but seeing an instruction repeatedly requires a number of episodes linear in the number of high-level instructions.

**Future Work.** This work considered high- and low-level synthetic language, but a more flexible framework could model a broad spectrum of abstraction, beyond two tiers. Moreover, future work could model the sequential order of relevant abstractions; in this work, we did not consider the information present in the order of relevant abstractions.

Highly diverse, compositional instructions remain a challenge. More sophisticated relevance classifiers could prove helpful: for example, rather than our current method of training the relevance classifier, we could maintain a belief distribution over whether a particular pair of high- and low-level instructions are relevant conditioned on trajectories the RL algorithm has observed so far.

## References

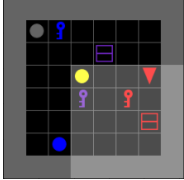
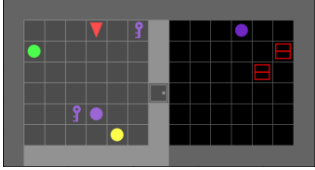
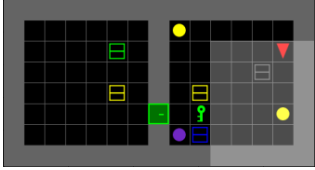
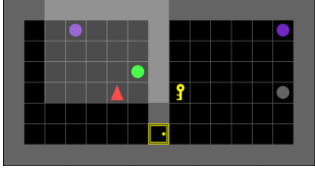
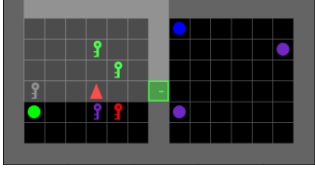
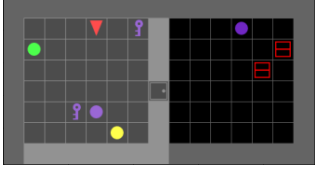
- Anderson, P., Wu, Q., Teney, D., Bruce, J., Johnson, M., Sünderhauf, N., Reid, I., Gould, S., and van den Hengel, A. Vision-and-language navigation: Interpreting visually-grounded navigation instructions in real environments. In *Computer Vision and Pattern Recognition (CVPR)*, 2018.
- Andreas, J., Klein, D., and Levine, S. Modular multitask reinforcement learning with policy sketches. In *International Conference on Machine Learning (ICML)*, 2017.
- Andrychowicz, M., Wolski, F., Ray, A., Schneider, J., Fong, R., Welinder, P., McGrew, B., Tobin, J., Abbeel, P., and Zaremba, W. Hindsight experience replay. *arXiv preprint arXiv:1707.01495*, 2017.
- Arumugam, D., Karamcheti, S., Gopalan, N., Wong, L. L. S., and Tellex, S. Accurately and efficiently interpreting human-robot instructions of varying granularities. In *Robotics: Science and Systems (RSS)*, 2017.
- Bahdanau, D., Hill, F., Leike, J., Hughes, E., Hosseini, S. A., Kohli, P., and Grefenstette, E. Learning to understand goal specifications by modelling reward. In *International Conference on Learning Representations (ICLR)*, 2019.
- Behboudian, P., Satsangi, Y., Taylor, M. E., Harutyunyan, A., and Bowling, M. Useful policy invariant shaping from arbitrary advice. *arXiv preprint arXiv:2011.01297*, 2020.
- Bisk, Y., Holtzman, A., Thomason, J., Andreas, J., Bengio, Y., Chai, J., Lapata, M., Lazaridou, A., May, J., Nisnevich, A., Pinto, N., and Turian, J. Experience grounds language. In *Empirical Methods in Natural Language Processing (EMNLP)*, 2020.
- Burda, Y., Edwards, H., Pathak, D., Storkey, A., Darrell, T., and Efros, A. A. Large-scale study of curiosity-driven learning. In *International Conference on Learning Representations (ICLR)*, 2019.
- Campero, A., Raileanu, R., Küttler, H., Tenenbaum, J. B., Rocktäschel, T., and Grefenstette, E. Learning with AMIGo: Adversarially motivated intrinsic goals. *arXiv preprint arXiv:2006.12122*, 2020.
- Chevalier-Boisvert, M., Bahdanau, D., Lahlou, S., Willems, L., Saharia, C., Nguyen, T. H., and Bengio, Y. BabyAI: A platform to study the sample efficiency of grounded language learning. In *International Conference on Learning Representations (ICLR)*, 2019.
- Cideron, G., Seurin, M., Strub, F., and Pietquin, O. Self-educated language agent with hindsight experience replay for instruction following. In *Advances in Neural Information Processing Systems (NeurIPS)*, 2019.
- Cobbe, K., Hesse, C., Hilton, J., and Schulman, J. Leveraging procedural generation to benchmark reinforcement learning. In *International Conference on Machine Learning (ICML)*, 2020.
- Colas, C., Karch, T., Lair, N., Dussoux, J., Moulin-Frier, C., Dominey, P. F., and Oudeyer, P. Language as a cognitive tool to imagine goals in curiosity driven exploration. In *Advances in Neural Information Processing Systems (NeurIPS)*, 2020.
- Das, A., Gkioxari, G., Lee, S., Parikh, D., and Batra, D. Neural modular control for embodied question answering. In *Conference on Robot Learning (CORL)*, 2018.
- Fu, J., Korattikara, A., Levine, S., and Guadarrama, S. From language to goals: Inverse reinforcement learning for vision-based instruction following. In *International Conference on Learning Representations (ICLR)*, 2019.
- Goyal, P., Niekum, S., and Mooney, R. J. Using natural language for reward shaping in reinforcement learning. In *International Joint Conference on Artificial Intelligence (IJCAI)*, 2019a.
- Goyal, Y., Shalit, U., and Kim, B. Explaining classifiers with causal concept effect (CaCE). *arXiv preprint arXiv:1907.07165*, 2019b.
- Grzes, M. Reward shaping in episodic reinforcement learning. In *International Conference on Autonomous Agents and Multiagent Systems (AAMAS)*, 2017.
- Hermann, K. M., Hill, F., Green, S., Wang, F., Faulkner, R., Soyer, H., Szepesvari, D., Czarnecki, W., Jaderberg, M., Teplyashin, D., Wainwright, M., Apps, C., Hassabis, D., and Blunsom, P. Grounded language learning in a simulated 3d world. *arXiv preprint arXiv:1706.06551*, 2017.

- Hill, F., Mokra, S., Wong, N., and Harley, T. Human instruction-following with deep reinforcement learning via transfer-learning from text. *arXiv preprint arXiv:2005.09382*, 2020.
- Jia, R. and Liang, P. Data recombination for neural semantic parsing. In *Association for Computational Linguistics (ACL)*, 2016.
- Jiang, Y., Gu, S. S., Murphy, K. P., and Finn, C. Language as an abstraction for hierarchical deep reinforcement learning. In *Advances in Neural Information Processing Systems (NeurIPS)*, 2019.
- Karamcheti, S., Williams, E. C., Arumugam, D., Rhee, M., Gopalan, N., Wong, L. L. S., and Tellex, S. A tale of two dragons: A hybrid approach for interpreting action-oriented and goal-oriented instructions. In *First Workshop on Language Grounding for Robotics @ ACL*, 2017.
- Karamcheti, S., Sadigh, D., and Liang, P. Learning adaptive language interfaces through decomposition. In *EMNLP Workshop for Interactive and Executable Semantic Parsing (IntEx-SemPar)*, 2020.
- Kollar, T., Tellex, S., Roy, D., and Roy, N. Toward understanding natural language directions. In *Human-Robot Interaction*, pp. 259–266, 2010.
- Luketina, J., Nardelli, N., Farquhar, G., Foerster, J., Andreas, J., Grefenstette, E., Whiteson, S., and Rocktäschel, T. A survey of reinforcement learning informed by natural language. In *International Joint Conference on Artificial Intelligence (IJCAI)*, 2019.
- Lynch, C. and Sermanet, P. Grounding language in play. *arXiv preprint arXiv:2005.07648*, 2020.
- McGovern, A. and Barto, A. G. Automatic discovery of sub-goals in reinforcement learning using diverse density. In *International Conference on Machine Learning (ICML)*, 2001.
- Misra, D. K., Langford, J., and Artzi, Y. Mapping instructions and visual observations to actions with reinforcement learning. In *Empirical Methods in Natural Language Processing (EMNLP)*, 2017.
- Ng, A. Y., Harada, D., and Russell, S. Policy invariance under reward transformations: Theory and application to reward shaping. In *International Conference on Machine Learning (ICML)*, volume 99, pp. 278–287, 1999.
- Pathak, D., Agrawal, P., Efros, A. A., and Darrell, T. Curiosity-driven exploration by self-supervised prediction. In *Computer Vision and Pattern Recognition (CVPR)*, pp. 16–17, 2017.
- Perez, E., Strub, F., Vries, H. D., Dumoulin, V., and Courville, A. C. Film: Visual reasoning with a general conditioning layer. In *Association for the Advancement of Artificial Intelligence (AAAI)*, 2018.
- Randløv, J. and Alstrøm, P. Learning to drive a bicycle using reinforcement learning and shaping. In *International Conference on Machine Learning (ICML)*, 1998.
- Schmidhuber, J. Adaptive confidence and adaptive curiosity. Technical report, Institut für Informatik, Technische Universität München, Arcisstr. 21, 800 München 2, 1991.
- Schulman, J., Wolski, F., Dhariwal, P., Radford, A., and Klimov, O. Proximal policy optimization algorithms. *arXiv preprint arXiv:1707.06347*, 2017.
- Shridhar, M., Thomason, J., Gordon, D., Bisk, Y., Han, W., Mottaghi, R., Zettlemoyer, L., and Fox, D. Alfred: A benchmark for interpreting grounded instructions for everyday tasks. In *Computer Vision and Pattern Recognition (CVPR)*, 2020.
- Stolle, M. and Precup, D. Learning options in reinforcement learning. In *Proceedings of the 5th International Symposium on Abstraction, Reformulation and Approximation*, 2002.
- Sutton, R. S., Precup, D., and Singh, S. Between mdps and semi-mdps: A framework for temporal abstraction in reinforcement learning. *Artificial intelligence*, 112:181–211, 1999.
- Tellex, S., Kollar, T., Dickerson, S., Walter, M. R., Banerjee, A. G., Teller, S. J., and Roy, N. Understanding natural language commands for robotic navigation and mobile manipulation. In *Association for the Advancement of Artificial Intelligence (AAAI)*, 2011.
- Thomason, J., Zhang, S., Mooney, R. J., and Stone, P. Learning to interpret natural language commands through human-robot dialog. In *International Joint Conference on Artificial Intelligence (IJCAI)*, 2015.
- Wang, S. I., Ginn, S., Liang, P., and Manning, C. D. Naturalizing a programming language via interactive learning. In *Association for Computational Linguistics (ACL)*, 2017.
- Wang, X. E., Huang, Q., Celikyilmaz, A., Gao, J., Shen, D., Wang, Y., Wang, W. Y., and Zhang, L. Reinforced cross-modal matching and self-supervised imitation learning for vision-language navigation. In *Computer Vision and Pattern Recognition (CVPR)*, 2019.
- Waytowich, N., Barton, S. L., Lawhern, V., and Warnell, G. A narration-based reward shaping approach using grounded natural language commands. In *International Conference on Machine Learning (ICML)*, 2019.
- Yu, H., Zhang, H., and Xu, W. A deep compositional framework for human-like language acquisition in virtual environment. *arXiv preprint arXiv:1703.09831*, 2017.

## A. Experiment Details

Table A provides additional reference information about our suite of evaluation tasks.

Table 2. Details of our low- and high-level tasks.

LOW-LEVEL TASK	# INSTR.	EXAMPLE	
GoTo-ROOM (G1)	36	<i>go to a red ball</i>	
GoTo-MAZE (G2)	42	<i>go to a red ball</i>	
OPEN-MAZE (O2)	6	<i>open the green door</i>	
PICK-MAZE (P2)	36	<i>pick up the blue box</i>	
HIGH-LEVEL TASK	# INSTR.	EXAMPLE	$\mathcal{G}_\ell$
PUTNEXT-ROOM	306	 <i>put the blue key next to the yellow ball</i>	G1
PUTNEXT-MAZE	1440	 <i>put the yellow ball next to a purple key</i>	G2
UNLOCK-MAZE	6	 <i>open the green door</i>	P2
OPEN&PICK-MAZE	216	 <i>open the yellow door and pick up the grey ball</i>	O2, G2
COMBO-MAZE	1266	 <i>pick up the green ball</i>	G2
SEQUENCE-MAZE	>1M	 <i>open the grey door after you put the yellow ball next to a purple key</i>	G2

## B. Training Details

We adapt the PPO implementation from (Chevalier-Boisvert et al., 2019) with their default hyperparameters (discount factor of 0.99, learning rate (via Adam) of  $7 \times 10^{-4}$ , batch size of 2560, minibatch size of 1280, entropy coefficient of 0.01, value loss coefficient of 0.5, clipping- $\epsilon$  of 0.2, and generalized advantage estimation parameter of 0.99). We use the actor-critic architecture from (Chevalier-Boisvert et al., 2019) (Figure 7).



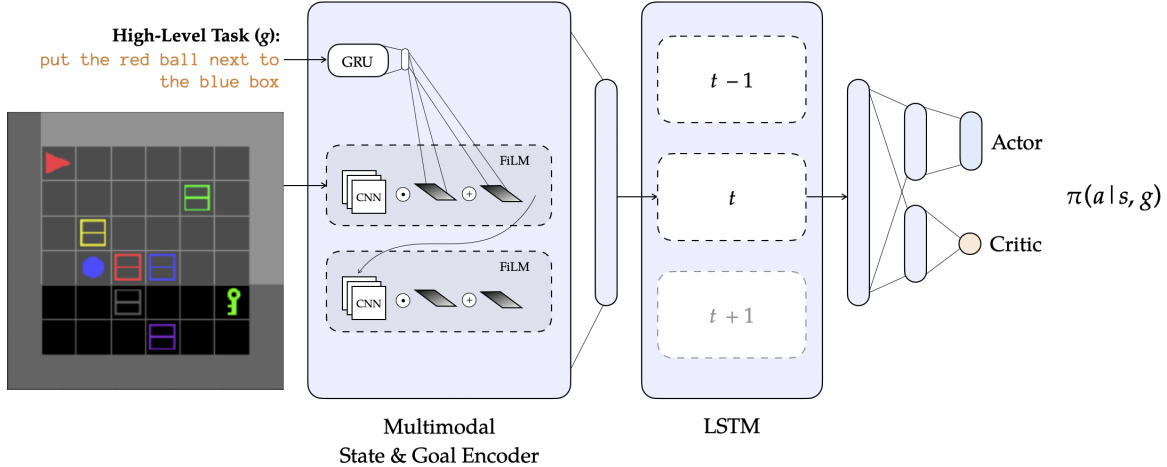


Figure 7. The actor-critic architecture processes an observation and language instruction using a multimodal encoder based on feature-wise linear modulation (FiLM) (Perez et al., 2018). It then uses an LSTM to recurrently process a history of observations and projects the output onto an actor head and a critic head.

### B.1. Termination and Relevance Classifiers

The termination classifier  $h^\phi$  is an adapted version of the architecture in Figure 7 that uses a binary prediction head instead of the actor and critic heads. Our implementation of  $h^\phi$  makes predictions based on single observations.

To train  $h^\phi$ , we require positive and negative examples of states at which low-level language instructions terminate. We use the automated expert built into BabyAI to generate 15K low-level episodes. For each episode, we use the final observation as a positive example for that episode’s language instruction and a randomly sampled state from the trajectory as a negative example. Similarly, we generate 200 episodes for validation data. We augment the datasets with additional negative examples by sampling 35 mismatching low-level instructions for each terminating observation. We use a batch size of 2560 and optimize via Adam with a learning rate of  $10^{-4}$ . We train for 5 epochs and use the iteration that achieves the highest validation accuracy.

We train the relevance classifier  $f^\rho$  online with the architecture described in Section 4. For an initialization conducive to deduplication and that provides  $\pi^\theta$  strong signal from the beginning of training, we initialize  $f^\rho$  to predict that all  $g_\ell$  are relevant for any  $g$ . To do this, we randomly sample 100 high-level instructions, cross that set with  $\mathcal{G}_\ell$ , label the pairs as relevant, and train for 20 epochs. We use a learning rate of  $10^{-4}$  and a batch size of 10. Online updates based on the online dataset  $\mathcal{D}$  involve 3 gradient updates to  $\rho$  for every 50 iterations of PPO.

### B.2. LEARN Baseline

We reimplement the LEARN model (Goyal et al., 2019a) based on an open-source implementation<sup>2</sup>. We collect 15K episodes of BabyAI’s automated expert completing low-level tasks and process them to create (*language instruction*, *action frequency*) data. We use this dataset to train the classifier used in LEARN which predicts whether the action frequencies of the current trajectory are related to the current language instruction. The coefficient on the shaped rewards is a hyperparameter of the method; based on an informed sweep of values, we set its value to 0.01. We train the classifier for 100 epochs.

An intuition for why LEARN has strong performance in static environments as in (Goyal et al., 2019b) but not in our setting is that the method requires action frequencies to provide a signal about whether the current trajectory is related to the language instruction. Our environments are dynamic, and so individual actions are less correlated to language tasks. Additionally, in our setting, the instructions during RL are high-level instructions which are selected from a different distribution than the low-level instructions available for training the classifier.

<sup>2</sup><https://github.com/prasoonogoyal/rl-learn>